

Surface Modification of Highly Oriented Pyrolytic Graphite Targets by Intense Pulsed Ion Beam Irradiation

Kenji Kashine, Tuneo Suzuki, Hisayuki Suematsu, Weihua Jiang, Kiyoshi Yatsui
and Yasuhiro Tanabe*

Extreme Energy-Density Research Institute, Nagaoka University of Technology, Nagaoka, Niigata 940-2188, Japan
Fax: +81-258-47-9890, e-mail: kashine@etigo.nagaokaut.ac.jp

*Materials and Structures Laboratory, Tokyo Institute of Technology, Yokohama, 226-8503, Japan
Fax: +81-45-924-5345, e-mail: tanabel@rlem.titech.ac.jp

High-density, high-pressure ablation plasma produced by intense pulsed ion beam has been used to modify the highly oriented pyrolytic graphite (HOPG) targets. The HOPG were irradiated by 60 - 120 J/cm² of pulsed proton beam. The sphere particles and whiskers were observed on the irradiated target surface by the scanning electron microscopy. In the Raman spectra of the irradiated HOPG targets, the intensity ratio of I_D/I_G was increased with increasing the beam energy density. In the X-ray diffraction patterns of the irradiated HOPG targets, the FWHM of 002 diffraction was broadened by the irradiation. We have understood that the graphite structure and crystallite size in the targets are considerably changed by the pulsed ion beam irradiation.

Key words: pulsed ion beam, high-density ablation plasma, surface modification, graphite whisker, Raman spectroscopy

1. INTRODUCTION

Pulsed ion beam has been found to be very efficient in generating high-density ablation plasma [1]. Such an ablation plasma has a variety of applications such as thin film deposition and foil acceleration [2,3].

When irradiates the pulsed ion beam to the target material, due to strong interaction with matter, ions can travel a very short distance in solid material. This distance is called range. Large amount of the ion beam energy was deposited in a very thin layer, whose thickness is comparable to the range. For instance, the range is only ~13 μm in carbon for the proton with the energy of 1 MeV. With this fast energy deposition, the heated surface layer immediately turns into high-density ablation plasma. In our previous works, we have studied the kinetics of the ablation plasma by the ion beam irradiated aluminum targets experiment [4,5]. Using the pressure and the temperature, we can expect the surface modification of the target materials. Furthermore, from these works, we have found that the pressure and the temperature are enhanced at the high energy density. Therefore, we can control pressure and temperature in the targets by changing the ion beam energy density on the target surface.

Carbon remains the major thermodynamically stable such as graphite, diamond, liquid and vapor phases. For example, in the phase diagram of carbon, triple point of graphite / diamond / liquid phase exists at ~12 GPa and ~5000 K. In solid state, i.e., graphite and diamond, there are two preferred form of electronic bonding such as sp² (graphite-like) and sp³ (diamond-like) of carbon atoms. Their physical properties strongly depend on the ratio of sp² and sp³ bonds. The ratio varies with synthesis conditions including temperature and pressure. Not only synthesis of bulk samples, but also modification of bulk surface of carbon have been performed by shock synthesis [6], ion implantation [7] and pulsed laser

irradiation [8,9]. As mentioned before, irradiation of target by pulsed ion beam also increases temperature and pressure in the vicinity of target surface. It is expected that surface modification of carbon targets by pulsed ion beam irradiation may be possible.

In this paper, we focus on the modification of the highly oriented pyrolytic graphite (HOPG) target surface due to the ablation plasma formed by the pulsed ion beam irradiation. The HOPG targets were irradiated with 60 ~ 120 J/cm² of pulsed ion beam. Behavior of the carbon plasma ablation was observed by high-speed camera. The morphology of the ablated surface was observed by scanning electron microscopy. The structure of irradiated targets was investigated by Raman spectroscopy and X-ray diffractometry.

2. EXPERIMENTAL SETUP

The ion-beam-irradiation experiments were carried out in a pulsed power generator, "ETIGO-II" [10].

Figure 1 illustrates the outline of the experimental setup using a magnetically insulated ion beam diode (MID)[11], which consists of the anode (inner electrode) and the cathode (outer electrode). The concave shaped anode has a flashboard (polyethylene) on its surface. The cathode has slits at its convex shaped front to extract ion beam. In addition, the cathode acts as a one-turn theta-pinch coil, where the current is supplied by an external power supply. The current in the cathode generates an insulating magnetic field between the cathode and the anode, by which the electrons are prevented from crossing the gap. On the other hand, the ions (approximately 75 % proton) are accelerated toward the cathode and focus toward the geometric center (d_{AT}=160 mm). The peak voltage of the diode was 1.1 MV. The pulse width was nearly 60 ns. The diode and the target chambers were pumped to pressure of ~2.6×10⁻² Pa during the experiments.

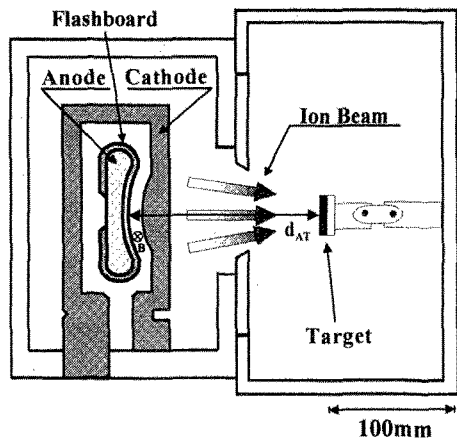


Fig.1 Experimental setup using a magnetically insulated ion beam diode (MID).

The ion beam energy density has been measured by a calorimeter method at various distance between the anode and the target material (d_{AT}). Figure 2 shows the average energy density of ion beam as a function of d_{AT} . The maximum average energy density of $\sim 120 \text{ J/cm}^2$ was obtained at d_{AT} of 150 mm. The energy density was decreased with increasing d_{AT} above 150 mm.

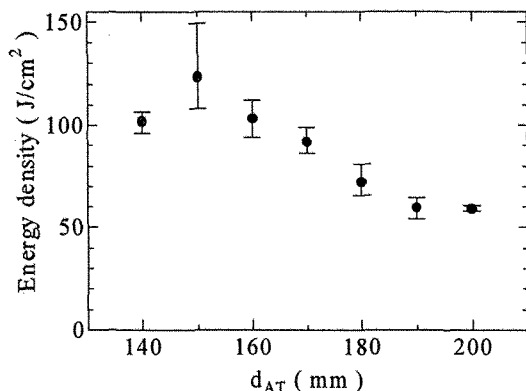


Fig.2 Ion energy density as a function of the anode-target distance.

Experimentally, the HOPG targets (Advanced Ceramics Corporation, Grade ZYH) were irradiated with $60 \sim 120 \text{ J/cm}^2$ of pulsed ion beam. One of the targets was set parallel to the cathode, and d_{AT} was changed at 150 and 180 mm. The number of shots for each target was one. Time evolution of the ablation plasma was observed by a high-speed camera (NAC Inc., ULTLA-NAC). The photograph configuration is 30 ns of exposure time and 500 ns of inter-frame. The morphology of the ablated surface was observed by scanning electron microscopy (SEM: JEOL, JSM-6700F). The samples before and after the irradiation were examined with a Raman spectrometer and an X-ray diffractometer. The Raman spectra were obtained using a Model Labram Infinity spectroscop (Jobin Yvon Co.), in backscattering mode using an argon-ion laser with the wavelength of 514.5 nm at power of 10 mW. The X-ray

diffractometer (RIGAKU, RINT2500PC) was utilized $\text{CuK}\alpha$ radiation of 0.15418 nm at the operating conditions of 50 kV and 300 mA. The incident angle α of X-ray to the target is fixed on the 5.0°

3. RESULTS AND DISCUSSIONS

Figure 3 shows high-speed photographs of the ablation plasma, where the energy density was $\sim 100 \text{ J/cm}^2$. The ion beam irradiates the target from right-hand-side and the ablation plasma expands in the direction perpendicular to the target surface. We confirmed the strongly plasma radiation on the target surface at the duration of first to fifth frame in Fig.3. The lifetime of the carbon plasma was several micro second.

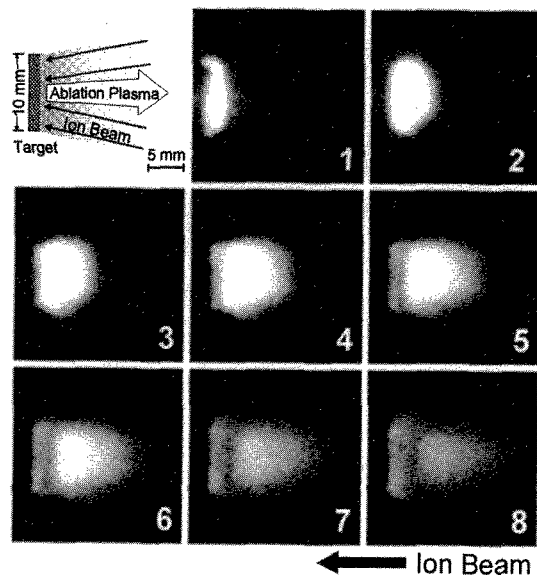


Fig.3 High-speed photographs of the carbon plasma formed by $\sim 100 \text{ J/cm}^2$ of ion beam irradiation.

Figure 4 shows SEM images of the surface of unirradiated (a) and irradiated (b) samples. Each sample was coated by Au sputtering to prevent the sample from the charging. The thickness of Au was $\sim 10 \text{ \AA}$. The irradiated sample was set at d_{AT} of 150 mm, i.e., the graphite target was irradiated with $\sim 120 \text{ J/cm}^2$ of ion beam (Fig.2). The observed area was the center of the irradiated region on the target surface. From Fig.4 (b), the irradiated sample has many sphere particles and whiskers. The size of these whiskers were nearly $1 \mu\text{m}$ in diameter.

There are two mechanisms to explain the growth of whiskers. One is the vapor-liquid-solid (VLS) mechanism which requires liquid droplets at the tips [12], and the other is the recrystallization growth mechanism which does not need the liquid droplets [13,14].

If the liquid droplet exists at the tip of the whisker, the VLS mechanism controls the growth process. In this mechanism, the liquid accepts material from the vapor, causing the liquid to become supersaturated. The liquid particle acts as the medium for transport from the vapor to the crystal and the whisker grows by precipitation of dissolved material from the droplet. In our experiment,

the cathode of MID was made of the stainless steel (SUS304). Hence, constituent element in SUS304 (Fe, Ni, Cr) was considerably existed on the target. Figure 5 represents the magnified image in the vicinity of Point A in Fig.4 (b) and an energy dispersive X-ray spectrometer (EDS) analysis result at Point A. From Fig.5, no constituent element in SUS304 was detected. It suggests the growth whisker by the VLS mechanism is not likely to take place in our experiment.

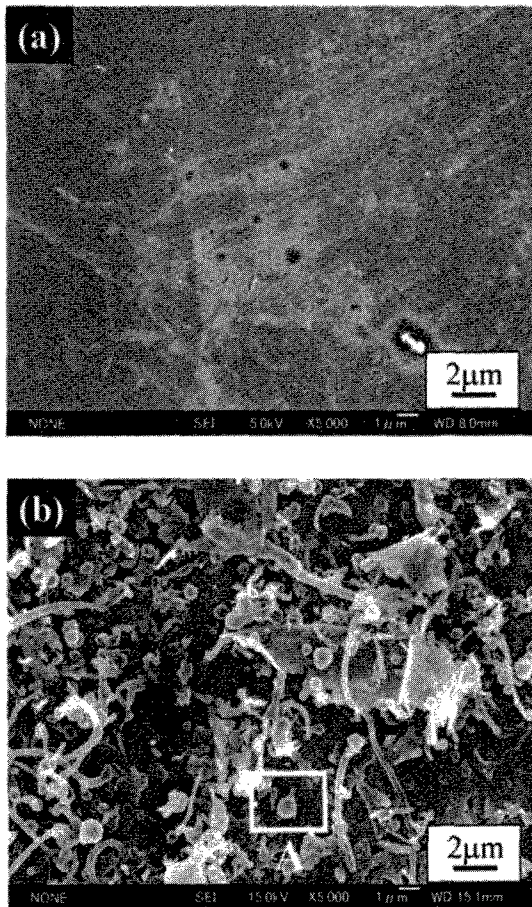


Fig.4 Surface of (a) unirradiated and (b) irradiated HOPG target observed by SEM.

According to Eshelby[13] and Furuta, et al. [14], the whisker took place by the extension of the free surface of a nucleating crystal either already present in the strained parent material or formed by recrystallization at the surface of the strained parent material. When the pulsed ion beam irradiates the target, the target surface has influenced with the fast heating and fast quenching effect by ablation plasma radiation [15]. Furthermore, the target has influenced with the high pressure effect by recoil of ablation plasma. Fisher[16] and Hasiguti[17] observed growth of whiskers from solid phase was enhanced with increasing hydraulic pressure. Hence, the whisker in Fig. 4(b) may be growing under hydraulic pressure, which was generated by the ablation plasma.

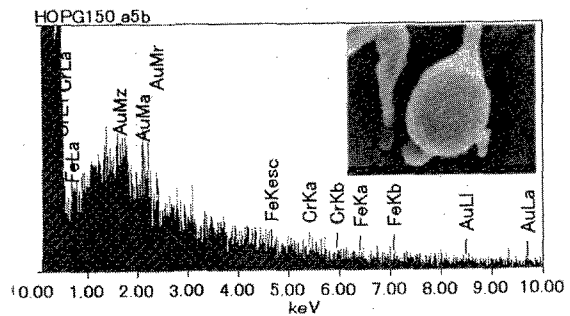


Fig.5 Magnified image in the vicinity of Point A in Fig.4 (b) and EDS analysis result at Point A.

The Raman spectroscopy was used to investigate the structure of irradiated targets. Figure 6 shows the typical Raman spectra of the irradiated targets. The observed area was the center of the irradiated region on the target surface. In the unirradiated target, the sharp peak can be observed in the spectrum at $\sim 1580 \text{ cm}^{-1}$ called G peak. The G peak corresponds to an in-plane vibration of graphite structure (E_{2g}), which is indicative of the presence of sp^2 bonds. In the irradiated target, the broad peak was observed in the spectrum at $\sim 1360 \text{ cm}^{-1}$ called D peak. The D peak corresponds to structural defects in graphite [18]. The FWHM and the ratio of the peak intensity of those peaks give us the information about the microstructure of the carbon material. In Fig.6, after the beam irradiation, the FWHM of the each peak was broadened and the intensity of D peak was increased. The intensity ratio of D peak to G peak (I_D/I_G) is increased with increasing the ion beam energy density.

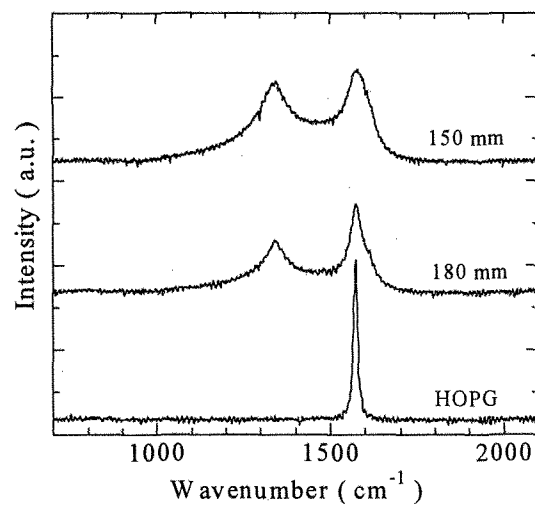


Fig.6 Raman spectra of the irradiated and unirradiated HOPG target.

On the Raman spectra of the graphite, many investigators have studied the relation between the peak-shift of the D or G peaks and disordering of the crystalstructure [19,20]. In our experiments, because of the D and G peaks were broad, no peak shift could be precisely measured. On the other hand, relative intensity of I_D increased with the increase in the ion beam energy

density. The degree of disordering was increased with increasing energy density of the ion beam.

Figure 7 shows the XRD patterns of graphite 002 diffraction. In the irradiated samples, the FWHM of the each peak are slightly broadened and shifted to the lower angle as the decrease in d_{AT} . This indicates that structure of graphite phase in the targets was slight changed by the ion beam irradiation.

From the X-ray diffraction results, we have two hypotheses for the structural change of graphite phase in the vicinity of the target surface. One is the decreasing of the graphite crystallite size in the c-direction (L_{002}) and another is the elongation of the graphite interlayer spacing (d_{002}). The broadening of the 002 peak as seen in Fig. 7 may be caused by the elongation of d_{002} because the broadening takes place only in the lower angle of the peak. The above consideration can be supported by the enhancement of I_D/I_G in Raman spectra (Fig. 6) with increasing the ion beam energy density.

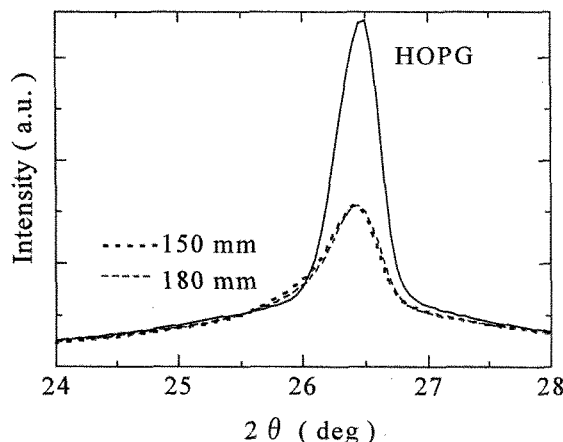


Fig.7 X-ray diffraction patterns of the irradiated and unirradiated HOPG target.

4. CONCLUSIONS

The surface modification experiments have been carried out on the highly oriented pyrolytic graphite targets by the pulsed ion-beam irradiation. The behavior of the carbon plasma was observed by high-speed photography. In the SEM image of the irradiated target, we observed sphere particles and whiskers which nearly 1 μm of diameter on the target surface. In the Raman spectra of the irradiated graphite targets, we see the intensity ratio of I_D/I_G was increased with increasing the beam energy density. In the X-ray diffraction patterns of the irradiated graphite targets, the FWHM of 002 diffraction was broadened by the irradiation. Considerable change in graphite structure and crystallite size took place by the ion beam irradiation.

ACKNOWLEDGEMENTS

This work was partly supported by a grant from the Ministry of Education, Culture, Sports, Science and Technology of Japan.

REFERENCES

- [1] K. Yatsui, *Laser and Part. Beams*, **7**, 733-741(1989).
- [2] K. Yatsui, C. Grigoriu, K. Masugata, W. Jiang and T. Sonegawa, *Jpn. J. Appl. Phys.*, **36**, 4928-4934 (1997).
- [3] K. Kashine, M. Yazawa, N. Harada, W. Jiang and K. Yatsui, *Jpn. J. Appl. Phys.*, **41**, 4014-4018 (2002).
- [4] K. Yatsui, H. Shinkai, K. Kashine, W. Jiang, M. Kagihiro and N. Harada, *Jpn. J. Appl. Phys.*, **40**, 955-959 (2001).
- [5] N. Harada, M. Yazawa, K. Kashine, W. Jiang and K. Yatsui, *Jpn. J. Appl. Phys.*, **40**, 960-964 (2001).
- [6] K. Yamada and Y. Tanabe, *Carbon*, **40**, 261-269 (2002).
- [7] B. S. Elman, M. Shayegan, M. S. Dresselhaus, H. Mazurek and G. Dresselhaus, *Phys. Rev. B*, **25**, 4142-4156 (1982).
- [8] M. D. Shirk and P. A. Molian, *Carbon*, **39**, 1183-1193 (2001).
- [9] A. Mechler, P. Heszler, Zs. Marton, M. Kovacs, T. Szorenyi and Z. Bor, *Appl. Surf. Sci.*, **154-155**, 22-28 (2000).
- [10] A. Tokuchi, N. Nakamura, T. Kunimatsu, N. Ninomiya, M. Den, A. Araki, K. Masugata and K. Yatsui, "Proc. 2nd Int. Topical Symp. on Inertial Confinement Fusion Research by High-Power Particle Beams", Ed. by K. Yatsui, Nagaoka University of Technology (1986) pp.430-439.
- [11] K. Yatsui, A. Tokuchi, H. Tanaka, H. Ishizuka, A. Kawai, E. Sai, K. Masugata, M. Ito and M. Matsui, *Laser and Part. Beams*, **3**, 119-155 (1985).
- [12] R. S. Wagner and W. C. Ellis, *Appl. Phys. Letters*, **4**, 89-90 (1964).
- [13] J. D. Eshelby, *Phys. Rev.*, **91**, 755-756 (1953).
- [14] N. Furuta and K. Hamamura, *Jpn. J. Appl. Phys.*, **8**, 1404-1410 (1969).
- [15] M. Yatsuzuka, Y. Hashimoto, T. Yamasaki and H. Uchida, *Jpn. J. Appl. Phys.*, **35**, 1857-1861 (1996).
- [16] R. M. Fisher, L. S. Darken and K. G. Carroll, *Acta metallurgica*, **2**, 368-373 (1954).
- [17] R. R. Hasiguti, *Acta metallurgica*, **3**, 200-201 (1955).
- [18] R. J. Nemanich and S. A. Solin, *Phys. Rev. B*, **20**, 392-401 (1979).
- [19] R. O. Dillon, J. A. Woollam and V. Katkanant, *Phys. Rev. B*, **29**, 3482-3489 (1984).
- [20] D. Beeman, J. Silverman, R. Lynds and M. R. Anderson, *Phys. Rev. B*, **30** 870-875 (1984).

(Received December 21, 2002; Accepted March 26, 2003)